

# Measuring velocity of sound with nuclear resonant inelastic x-ray scattering

M. Y. Hu,<sup>1,\*</sup> W. Sturhahn,<sup>2</sup> T. S. Toellner,<sup>2</sup> P. Mannheim,<sup>3</sup> D. E. Brown,<sup>4</sup> J. Zhao,<sup>2</sup> and E. E. Alp<sup>2</sup>

<sup>1</sup>*HP-CAT and Carnegie Institution of Washington, Advanced Photon Source, Argonne, IL 60439*

<sup>2</sup>*Advanced Photon Source, Argonne National Laboratory, Argonne, IL 60439*

<sup>3</sup>*Department of Physics, University of Connecticut, Storrs, CT 06269*

<sup>4</sup>*Department of Physics, Northern Illinois University, DeKalb, IL 60115*

(Dated: Dec. 13, 2002)

Nuclear resonant inelastic x-ray scattering is used to measure the projected partial phonon density of states of materials. A relationship is derived between the low-energy part of this frequency distribution and the sound velocity of materials. Our derivation is valid for harmonic solids with Debye-like low-frequency dynamics. This method of sound velocity determination is applied to elemental, composite, and impurity samples which are representative of a wide variety of both crystalline and noncrystalline materials. Advantages and limitations of this method are elucidated.

PACS numbers: 61.10.Eq, 62.65.+k

Mechanical properties form an important part of our understanding of condensed matter. In many areas of science, measurements of sound velocity are used to study materials of both natural occurrence and artificial fabrications. For example, in the field of geophysics, the sound velocity is the most direct information we have about the Earth's interior. The standard approach to learn about the composition and structure of the Earth's interior entails measurements of sound velocities of candidate compounds. The results are then compared to seismological data to exclude or confirm a particular compound. In the following, we will describe the use of nuclear resonant inelastic x-ray scattering (NRIXS) to measure the velocity of sound.

The NRIXS method was introduced to probe the lattice dynamics of materials by employing low-energy nuclear resonances.<sup>1,2</sup> In NRIXS experiments, only signals from nuclear resonance absorption are monitored, and for this reason the extracted quantity is specific to the resonant isotope. This technique provides the phonon excitation spectrum as seen by the probe nuclei,<sup>3,4,5</sup> and in most cases one can extract the partial vibrational frequency distribution, a function often referred to as the partial phonon density of states (PDOS). The NRIXS method has been applied to various materials, e.g., thin films and multilayers,<sup>6,7,8</sup> nanoparticles,<sup>9,10</sup> crystals with impurities,<sup>11</sup> organic molecules,<sup>12,13,14,15</sup> proteins,<sup>16,17</sup> samples under high pressures,<sup>18</sup> and samples of geophysical interests.<sup>19,20</sup> Most of these samples are compounds, and, while the obtained PDOS gives only part of the lattice dynamics, the low-energy portion of the PDOS provides the Debye sound velocity of the whole sample. We will now show that, due to universal features of acoustic modes of harmonic solids, the low-energy portion of the PDOS is related to the Debye sound velocity in a simple way.

The normalized phonon density of states is defined by

$$\nu(E) = \frac{1}{3N} \sum_l^{3N} \delta(E - E_l) , \quad (1)$$

where the energy eigenstates of lattice vibrations  $E_l$  are labeled by quantum number  $l$ , and  $N$  is the total number of atoms in the solid. In the harmonic lattice approximation, a PDOS, which is more relevant to NRIXS experiments, is given by<sup>3</sup>

$$\mathcal{D}(E, \hat{\mathbf{k}}) = \frac{1}{\tilde{N}} \sum_{\nu=1}^{\tilde{N}} \frac{1}{N} \sum_{l=1}^{3N} |\hat{\mathbf{k}} \cdot \mathbf{e}_l^{\nu}|^2 \delta(E - E_l) , \quad (2)$$

where  $\nu$  enumerates resonant nuclei,  $\tilde{N}$  is the total number of resonant nuclei,  $\hat{\mathbf{k}}$  is a unit vector in the incident photon direction, and  $\mathbf{e}_l^{\nu}$  are phonon polarization vectors. Equation (2) shows that the vibrational polarizations are projected onto the incident photon direction and in particular the vibrational modes with polarization perpendicular to the direction of the incident photon do not contribute. In the case of a single crystal, the measured vibrational properties become dependent on the incident photon direction and were called “projected,”<sup>21,22</sup> whereas in cases of polycrystalline or isotropic samples, the measured spectrum is an average over all directions. For a crystal in which resonant nuclei occupy only equivalent lattice sites, the quantity that can be extracted from NRIXS experiments is exactly described by Eq. (2). When the resonant nuclei occupy different sites, what can be extracted is an approximation of Eq. (2). The approximation is based on an average of phonon spectra for these different lattice sites. The closure conditions of the phonon polarization vectors guarantee the normalization of  $\mathcal{D}(E, \hat{\mathbf{k}})$ , i.e., its integration over all phonon energies is one. The orthonormality and closure conditions are given by

$$\frac{1}{N} \sum_{\mu=1}^N (\mathbf{e}_l^{\mu})^* \cdot \mathbf{e}_{l'}^{\mu} = \delta_{ll'} , \quad (3)$$

$$\frac{1}{N} \sum_{l=1}^{3N} (e_l^{\mu\alpha})^* e_l^{\nu\beta} = \delta_{\mu\nu} \delta_{\alpha\beta} , \quad (4)$$

where  $\alpha, \beta$  denote the spatial components. These conditions hold for any harmonic solid, and the polarization

vectors have to be specified for every atom in the solid, in contrast to the crystal case, where they only need to be specified for the small number of atoms in a unit cell. The deviation of  $D(E, \hat{\mathbf{k}})$  from  $\nu(E)$  is contained in the behavior of the phonon polarization vectors  $\mathbf{e}_l^\mu$  and can be expressed in terms of a modulating function,

$$\mathcal{D}(E, \hat{\mathbf{k}}) = \chi(E, \hat{\mathbf{k}}) \nu(E), \quad (5)$$

which we now determine for low-energy vibration modes.

In a crystal, the acoustic modes form three branches described by phonon momentum. For disordered solids, we still expect hydrodynamic modes on length scales that are large compared to length scales characterized by inhomogeneities in the material. In the appendix, we discuss the properties of such hydrodynamic modes. Our results show that linearly dispersing plane-wave modes exist on long length scales, and that these modes are described by momentum  $\mathbf{q}$  and branch number  $s$ . Energies and atomic displacements associated with these modes take the following form

$$\begin{aligned} E_{\mathbf{q}s} &= c_{\hat{\mathbf{q}}s} \hbar q \\ \mathbf{u}_{\mathbf{q}s}^\mu &= \alpha_{\mathbf{q}s} \hat{\mathbf{p}}_{\hat{\mathbf{q}}s} e^{i\mathbf{q}\cdot\mathbf{r}_\mu}, \end{aligned} \quad (6)$$

where  $c_{\hat{\mathbf{q}}s}$  is the sound velocity,  $\hat{\mathbf{p}}_{\hat{\mathbf{q}}s}$  is a normalized polarization vector, and  $\mathbf{r}_\mu$  are the atomic positions. The normalization factor  $\alpha_{\mathbf{q}s}$  can be determined as follows. If a normal mode  $l$  contains the energy  $E_l$ , the atomic displacements are given by<sup>3</sup>

$$\mathbf{u}_l^\mu = \frac{\hbar}{\sqrt{2m_\mu E_l}} \mathbf{e}_l^\mu, \quad (7)$$

where  $\mathbf{e}_l^\mu$  are phonon polarization vectors introduced in Eq. (2) and  $m_\mu$  is the mass of atom  $\mu$ . A comparison with Eq. (6) under consideration of the normalization condition Eq. (3) results in  $\alpha_{\mathbf{q}s} = \hbar / \sqrt{2m E_{\mathbf{q}s}}$ , where  $m$  is the average atomic mass. For the low-energy, hydrodynamic modes, we can therefore write

$$\mathbf{e}_l^\mu = \mathbf{e}_{\mathbf{q}s}^\mu = \sqrt{\frac{m_\mu}{m}} \hat{\mathbf{p}}_{\hat{\mathbf{q}}s} e^{i\mathbf{q}\cdot\mathbf{r}_\mu}. \quad (8)$$

In the small  $q$ , low-energy regime, we rewrite Eq. (2) by replacing the summation over phonon modes with an integration,  $\sum_l \rightarrow V/(2\pi)^3 \sum_s \int q^2 d\mathbf{q} d\Omega_q$ , and we substitute Eqs. (6) and (8) into Eq. (2) to obtain

$$\chi(\hat{\mathbf{k}}) = \frac{\tilde{m}}{m} v_D^3 \sum_{s=1}^3 \int \frac{d\Omega_q}{4\pi} \frac{(\hat{\mathbf{k}} \cdot \hat{\mathbf{p}}_{\hat{\mathbf{q}}s})^2}{c_{\hat{\mathbf{q}}s}^3}, \quad (9)$$

where  $\tilde{m}$  is the mass of the nuclear resonant isotope, and the Debye velocity  $v_D$  is defined as an average over all sound velocities

$$\frac{1}{v_D^3} = \frac{1}{3} \sum_{s=1}^3 \int \frac{d\Omega_q}{4\pi} \frac{1}{c_{\hat{\mathbf{q}}s}^3}. \quad (10)$$

If we define a projected sound velocity similarly by

$$\frac{1}{v_{\hat{\mathbf{k}}}^3} = \sum_{s=1}^3 \int \frac{d\Omega_q}{4\pi} \frac{(\hat{\mathbf{k}} \cdot \hat{\mathbf{p}}_{\hat{\mathbf{q}}s})^2}{c_{\hat{\mathbf{q}}s}^3}, \quad (11)$$

we obtain the simple relationship

$$\chi(\hat{\mathbf{k}}) = \frac{\tilde{m}}{m} \left( \frac{v_D}{v_{\hat{\mathbf{k}}}} \right)^3. \quad (12)$$

For small energies, the modulating function becomes energy independent. For an isotropic sample, the sound velocity does not have directional dependence, and we can further simplify Eq. (11) to obtain  $v_{\hat{\mathbf{k}}} = v_D$ . In the case of a polycrystalline sample, averaging over all nuclear resonant sites in Eq. (2) is equivalent to averaging Eq. (9) over all directions of  $\mathbf{k}$ . Thus, in both cases, we have

$$\chi = \frac{\tilde{m}}{m}. \quad (13)$$

Finally, for an isotropic or a polycrystalline sample, in the low-energy regime Eq. (2) becomes

$$\mathcal{D}(E) = \left( \frac{\tilde{m}}{m} \right) \frac{E^2}{2\pi^2 \hbar^3 n v_D^3}, \quad (14)$$

where  $n$  is the density of atoms. Equation (14) has appeared in a similar form in a NRIXS study of myoglobin and related biological compounds.<sup>17</sup> Here we have given a derivation of Eqs. (13) and (14), and for low-energy modes the required modulation function  $\chi(E, \hat{\mathbf{k}})$  is given by the mass ratio  $\tilde{m}/m$ . In addition, Eq. (12) shows the dependence of the modulation function on the photon direction for anisotropic samples.

The PDOS of a variety of samples has been measured by NRIXS. Here we show three examples representing crystals (bcc iron, hematite) and materials with point defects (<sup>119</sup>Sn<sub>0.01</sub>Pd<sub>0.99</sub>). The crystalline samples are translationally invariant, and thus for them the basis of modes is in fact given by momentum eigenstates with polarization vectors which are known to obey Eq. (8) explicitly.<sup>23</sup> While the point-defect case is expressly not translationally invariant, by using the lattice Green's function technique, it is still possible to find closed form expressions for the polarization vectors, with Eqs. (13) and (14) again being found to follow. We shall describe the details of this specific calculation elsewhere,<sup>24</sup> while noting here that the modulation to the host lattice DOS is found to depend only on the mass ratio even in the event of a force constant change at the defect site.<sup>25</sup>

The low-energy region of the PDOS divided by energy squared is displayed for the three samples in Fig. 1. Bcc iron 95% enriched in <sup>57</sup>Fe is an example of the limiting case where  $\tilde{N} \sim N$ , and NRIXS provides the total rather than the partial DOS. Hematite enriched with <sup>57</sup>Fe represents a situation, in which the resonant nuclei form only a part of the unit cell. The <sup>119</sup>Sn<sub>0.01</sub>Pd<sub>0.99</sub> sample represents another limiting case in which the nuclear resonant

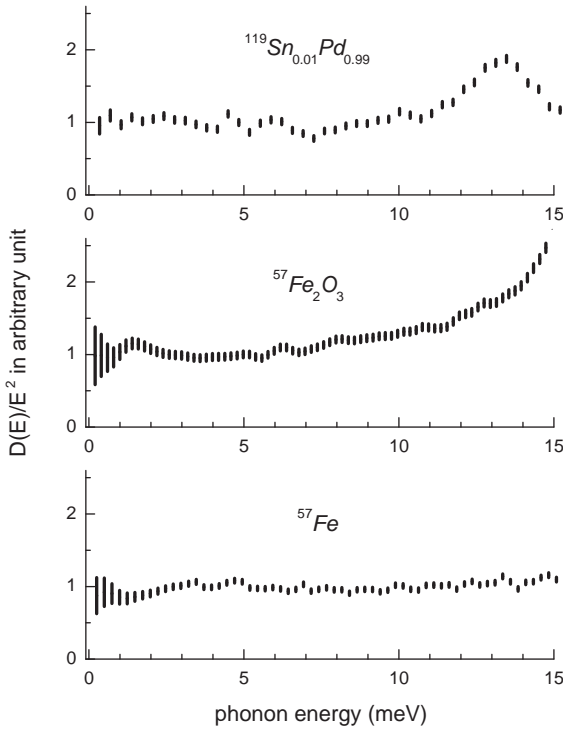


FIG. 1: The measured PDOS divided by energy squared. The size of symbols indicates the statistical error bar derived from signal counts. These samples were measured with resolutions of 0.85 meV for  $^{119}\text{Sn}_{0.01}\text{Pd}_{0.99}$ , 0.6 meV for  $^{57}\text{Fe}_2\text{O}_3$ , and 1 meV for bcc iron.

isotopes occupy only a very small portion of the lattice sites. In this limit,  $\tilde{N} \ll N$ , the average atomic mass  $m$  in the above equations is well approximated by the mass of a host lattice atom. The analog of Eq. (14) is derived in a Green's function treatment of the dynamics of a point defect.<sup>24</sup> These samples thus represent a very broad range of nuclear resonant isotope concentrations.

We extracted numerical values for the velocities of sound by averaging  $D(E)/E^2$  obtained from measured data in the region from zero to 5 meV according to Eq. (14). The results are tabulated in Table I, where we also compare our values with sound velocities from other sources as explained in the footnotes of the table. For iron and palladium, the results from NRIXS measurements are within the range of sound velocities that were obtained by other means. In the case of hematite, our results give clearly a lower value for  $v_D$  than is obtained from the measured elastic constants. It is difficult for us to judge the reliability of values for  $v_D$  obtained by other methods that usually do not measure  $v_D$  directly but rely on post-experimental data averaging. Values obtained with the NRIXS method seem to be lower or on the lower end of ranges given by other authors. This might be due to the fact that the phonon spectrum up to 5 meV corresponding to a frequency of 1.2 THz is used

TABLE I: Comparison of velocities of sound, together with the factor  $(\tilde{m}/m)$  in Eqs. (13) and (14).

	velocity of sound (m/s)	$\tilde{m}/m$
Palladium	$2193 \pm 35^a$	1.12
	$2104^b$	
	$2372^c$	
Hematite	$4279 \pm 84^a$	1.76
	$4653^d$	
Iron	$3488 \pm 48^a$	1.00
	$3412^b$	
	$3707^c$	

<sup>a</sup>Our results from NRIXS.

<sup>b</sup>The lower limits from ref. 30.

<sup>c</sup>The upper limits from ref. 30.

<sup>d</sup>Calculated with bulk and shear moduli from ref. 31.

to derive the sound velocity. At such high frequencies, the phonon dispersion may already be nonlinear, which would typically lead to a reduction in the value of the obtained  $v_D$ . Improvements in energy resolution could make smaller phonon energies accessible, which would potentially provide a better measure of sound velocity.

We have relied critically on the assumption of Debye behavior at small phonon energies. In particular, we require Debye behavior to extrapolate to typical sound frequencies ( $10^4$  Hz) from the THz range, which is accessible to NRIXS. However, in Fig. 1, we see deviations from Debye behavior, which would correspond to a horizontal line. Besides nonlinearities in the phonon dispersion as mentioned above, the removal of the elastic contributions to the NRIXS spectra can be a source of systematic uncertainties.<sup>5,26,27</sup> Also the NRIXS technique relies on harmonic behavior of the sample to extract the PDOS from the measured data.<sup>26,27</sup> All these possibilities may contribute to the deviations seen in Fig. 1. In future studies aimed at low-frequency dynamics, we suggest measuring the resolution function simultaneously by nuclear forward scattering to improve the reliability of peak subtraction. In any case, a highly accurate resolution function should be available. Besides the peak-subtraction procedure and the energy resolution (usually defined as FWHM), the shape of the resolution function is also of major importance. The access to small excitation energies is greatly improved if the tails of the resolution function can be minimized by design of the x-ray monochromator.<sup>28</sup> Furthermore, difficulties in the peak removal usually become more severe with increasing ratio of elastic to inelastic scattering intensities. In many cases, the relative strength of the elastic scattering is reduced by saturation effects in the sample.<sup>2</sup> This highly desirable effect is less pronounced for samples with low concentrations of the resonant isotope or in cases of generally weak inelastic scattering, e.g., at very low temperatures. In addition to the special requirements for data collection near the elastic peak, an accurate mea-

surement of the entire spectrum is equally important to achieve an accurate normalization.

We have shown that nuclear resonant isotopes can be used to measure the sound velocity of a solid in the context of the harmonic approximation and Debye-like low-frequency dynamics. Our approach is valid even for very low concentrations of the nuclear resonant isotope, and therefore the probing nuclei provide information about the host lattice. We expect that the presented method will have significant impact in the scientific area of high-pressure research and, in particular, in the field of geo-physics, where sound velocity is of great interest. Also the strategic placement of resonant nuclei in artificial structures may provide insight into local atomic motion, which at low energies is thought to influence the electronic noise in nanostructure devices. Thus NRIXS opens another venue to measure sound velocities of solids and can complement other techniques or even supercede established methods in those cases, where they become too demanding or even impossible.

This work and use of the Advanced Photon Source are supported by the U.S. Department of Energy, Basic Energy Sciences, Office of Science, under contract No. W-31-109-ENG-38, and by the State of Illinois under HECA.

## Appendix

Our study of long-wavelength vibrational excitations starts with the continuum version of the equations of motion of a set of harmonically bound atoms, which reads

$$\omega^2 m^\mu \mathbf{u}^\mu = - \sum_\nu \Phi^{\mu\nu} \mathbf{u}^\nu , \quad (15)$$

where  $\Phi^{\mu\nu}$  are the force constant matrices and  $\mathbf{u}^\mu$  is the displacement vector of atom  $\mu$  for a vibrational mode of energy  $\hbar\omega$ . We introduce mass and atomic density functions  $\rho(\mathbf{x})$  and  $\eta(\mathbf{x})$  by

$$\begin{aligned} \rho(\mathbf{x}) &= \sum_\mu m^\mu \delta^3(\mathbf{x} - \mathbf{r}_\mu) \\ \eta(\mathbf{x}) &= \sum_\mu \delta^3(\mathbf{x} - \mathbf{r}_\mu) , \end{aligned} \quad (16)$$

where  $\mathbf{r}_\mu$  is the position of atom  $\mu$ . The continuum version that substitutes Eq. (15) is then given by

$$\omega^2 \rho(\mathbf{x}) \mathbf{u}(\mathbf{x}) = - \int \eta(\mathbf{x}) \Phi(\mathbf{x} - \mathbf{x}') \eta(\mathbf{x}') \mathbf{u}(\mathbf{x}') d^3 x' , \quad (17)$$

where we made the usual assumption that the force constant matrix depends on coordinate differences only. The original intentions to study long-wavelength excitations are served best by introducing Fourier transforms, e.g.,  $\tilde{\mathbf{u}}(\mathbf{q}) = FT[\mathbf{u}(\mathbf{x})]$ , and eventually expanding for small values of momentum. The transformed Eq. (17) reads

$$\omega^2 \int \tilde{\rho}(\mathbf{q} - \mathbf{q}') \tilde{\mathbf{u}}(\mathbf{q}') d^3 q' = - \frac{1}{(2\pi)^3} \times$$

$$\int \tilde{\eta}(\mathbf{q} - \mathbf{q}') \tilde{\Phi}(\mathbf{q}') \tilde{\eta}(\mathbf{q}' - \mathbf{q}'') \tilde{\mathbf{u}}(\mathbf{q}'') d^3 q' d^3 q'' \quad (18)$$

The quantities  $\tilde{\eta}(\mathbf{q})$  and  $\tilde{\rho}(\mathbf{q})$  are closely related to the structure function  $S(\mathbf{q})$  that is typically obtained from x-ray or neutron diffraction experiments. For crystals, these functions are described by a series of very sharp peaks at values given by the reciprocal lattice vectors. Disordered or amorphous materials do not produce these sharp peaks with the exception of the  $\mathbf{q} = 0$  maximum which is not related to spatial order. One can assume that some of the salient features of Eq. (18) are captured by retaining the  $\mathbf{q} = 0$  maximum only, i.e., we approximate

$$\begin{aligned} \tilde{\rho}(\mathbf{q}) &= (2\pi)^3 \frac{m}{V} \delta^3(\mathbf{q}) \\ \tilde{\eta}(\mathbf{q}) &= (2\pi)^3 \frac{1}{V} \delta^3(\mathbf{q}) , \end{aligned} \quad (19)$$

where  $m$  and  $V$  are the average mass and volume per atom. Equation (18) simplifies to

$$m \omega^2 \tilde{\mathbf{u}}(\mathbf{q}) = - \frac{1}{V} \tilde{\Phi}(\mathbf{q}) \tilde{\mathbf{u}}(\mathbf{q}) , \quad (20)$$

and describes a class of solutions that should be common for all harmonic solids. The previous equation permits us to label the modes with the value of  $\mathbf{q}$  and a branch index  $s$  originating from the tensor character of the force-constant matrix, i.e.,  $\omega = \omega_{qs}$ . We note that  $\tilde{\Phi}(0) = 0$  follows from the invariance of the vibrational energy with respect to a displacement identical for all atoms. Assuming that the force-constant matrix falls off sufficiently fast with distance an expansion of Eq. (20) in powers of  $q = |\mathbf{q}|$  is permissible. The first-order term in this expansion will also vanish under the reasonable assumption of inversion symmetry of the force-constant matrix. For hydrodynamic modes, i.e.,  $q \rightarrow 0$ , we may therefore use

$$\tilde{\Phi}(\mathbf{q}) = \frac{q^2}{2} \left( \frac{\partial^2 \tilde{\Phi}}{\partial q^2} \right)_{q=0} , \quad (21)$$

and long-wavelength vibrational excitations are described by a modified Eq. (20)

$$m \omega_{qs}^2 \tilde{\mathbf{u}}(\mathbf{q}) = q^2 \tilde{\Theta}(\hat{\mathbf{q}}) \tilde{\mathbf{u}}(\mathbf{q}) . \quad (22)$$

We obtain linearly dispersing modes with energies  $\hbar\omega_{qs} = c_{\hat{\mathbf{q}}s} \hbar q$  with sound velocities  $c_{\hat{\mathbf{q}}s}$  that depend on the direction of  $\mathbf{q}$ . The matrix  $\tilde{\Theta}$  is related to the elastic tensor of the material (see for example ref. 29) and is given by

$$\tilde{\Theta}(\hat{\mathbf{q}}) = - \frac{1}{2V} \left( \frac{\partial^2 \tilde{\Phi}}{\partial q^2} \right)_{q=0} = \frac{1}{2N} \sum_\mu (\hat{\mathbf{q}} \cdot \mathbf{r}_\mu)^2 \Phi(\mathbf{r}_\mu) . \quad (23)$$

$N$  is the number of atoms in the sample. The eigenvalues of  $\tilde{\Theta}$  provide us with the sound velocities, and the

corresponding eigenvectors will not depend on  $q$ . The displacement field for a mode  $\mathbf{q}_s$  is then given by

$$\mathbf{u}_{\mathbf{q}_s}^{\mu} = \alpha_{\mathbf{q}_s} \mathbf{p}_{\hat{\mathbf{q}}_s} e^{i\mathbf{q}_s \cdot \mathbf{r}_{\mu}} , \quad (24)$$

where  $\hat{\mathbf{p}}_{\hat{\mathbf{q}}_s}$  is a normalized eigenvector of  $\tilde{\Theta}$  describing the polarization of the mode, and  $\alpha_{\mathbf{q}_s}$  is an appropriately

chosen normalization factor. Equation (24) shows that, even for disordered materials, hydrodynamic modes are equivalent to plane-wave excitations of the atomic displacements.

\* Electronic address: myhu@anl.gov

- <sup>1</sup> M. Seto, Y. Yoda, S. Kikuta, X. W. Zhang, and M. Ando, Phys. Rev. Lett. **74**, 3828 (1995).
- <sup>2</sup> W. Sturhahn, T. S. Toellner, E. E. Alp, X. Zhang, M. Ando, Y. Yoda, S. Kikuta, M. Seto, C. W. Kimball, and B. Dabrowski, Phys. Rev. Lett. **74**, 3832 (1995).
- <sup>3</sup> W. Sturhahn and V. G. Kohn, Hyperfine Interactions **123/124**, 367 (1999).
- <sup>4</sup> A. I. Chumakov and W. Sturhahn, Hyperfine Interactions **123/124**, 781 (1999).
- <sup>5</sup> M. Y. Hu, W. Sturhahn, T. S. Toellner, P. M. Hession, J. P. Sutter, and E. E. Alp, Nucl. Instrum. Methods A **428**, 551 (1999).
- <sup>6</sup> R. Röhlsberger, W. Sturhahn, T. S. Toellner, K. W. Quast, P. Hession, M. Hu, J. Sutter, and E. E. Alp, J. Appl. Phys. **86**, 584 (1999).
- <sup>7</sup> W. Keune and W. Sturhahn, Hyperfine Interactions **123/124**, 847 (1999).
- <sup>8</sup> B. Roldan-Cuenya, W. Keune, W. Sturhahn, T. S. Tollner, and M. Y. Hu, Phys. Rev. B, **64**, 235321 (2001).
- <sup>9</sup> B. Fultz, C. C. Ahn, E. E. Alp, W. Sturhahn, and T. S. Toellner, Phys. Rev. Lett. **79**, 937 (1997).
- <sup>10</sup> L. Pasquini, A. Barla, A. I. Chumakov, O. Leupold, R. Rüffer, A. Deriu, and E. Bonetti, Phys. Rev. E **66**, 073410 (2002).
- <sup>11</sup> M. Seto, Y. Kobayashi, S. Kitao, R. Haruki, T. Mitsui, Y. Yoda, S. Nasu, and S. Kikuta, Phys. Rev. B **61**, 11420 (2000).
- <sup>12</sup> H. Paulsen, H. Winkler, A. X. Trautwein, H. Grünsteudel, V. Rusanov, and H. Toftlund, Phys. Rev. E **59**, 975 (1999).
- <sup>13</sup> H. Paulsen, R. Benda, C. Herta, V. Schünemann, A. I. Chumakov, L. Duelund, H. Winkler, H. Tolflund, and A. X. Trautwein, Phys. Rev. Lett. **86**, 1351 (2001).
- <sup>14</sup> B. K. Rai, S. M. Durbin, E. W. Prohofsky, J. T. Sage, G. R. A. Wyllie, W. R. Scheidt, W. Sturhahn, and E. E. Alp, Biophys. J. **82**, 2951 (2002).
- <sup>15</sup> B. K. Rai, S. M. Durbin, E. W. Prohofsky, J. T. Sage, M. K. Ellison, W. R. Scheidt, W. Sturhahn, and E. E. Alp, Phys. Rev. E **66**, 051904 (2002).
- <sup>16</sup> J. T. Sage, S. M. Durbin, W. Sturhahn, D. C. Wharton, P. M. Champion, P. Hession, J. P. Sutter, and E. E. Alp, Phys. Rev. Lett. **86**, 4966 (2001).
- <sup>17</sup> K. Achterhold, C. Keppler, A. Ostermann, U. van Bürck, W. Sturhahn, E. E. Alp, and F. G. Parak, Phys. Rev. E **65**, 051916 (2002).
- <sup>18</sup> V. V. Struzhkin, H.-K. Mao, J. Hu, M. Schwoerer-Böhning, J. Shu, R. J. Hemley, W. Sturhahn, M. Y. Hu, E. E. Alp, P. Eng, et al., Phys. Rev. Lett. **87**, 255501 (2001).
- <sup>19</sup> R. Lübbers, H. F. Grünsteudel, A. I. Chumakov, and G. Wortmann, Science **287**, 1250 (2000).
- <sup>20</sup> H. K. Mao, J. Xu, V. V. Struzhkin, J. Shu, R. J. Hemley, W. Sturhahn, M. Y. Hu, E. E. Alp, L. Vocadlo, D. Alfe, et al., Science **292**, 914 (2001).
- <sup>21</sup> A. I. Chumakov, R. Rüffer, A. Q. R. Baron, H. Grünsteudel, H. F. Grünsteudel, and V. G. Kohn, Phys. Rev. E **56**, 10758 (1997).
- <sup>22</sup> V. G. Kohn, A. I. Chumakov, and R. Rüffer, Phys. Rev. E **58**, 8437 (1998).
- <sup>23</sup> A. A. Maradudin, E. W. Montroll, G. H. Weiss, and I. P. Ipatova, *Theory of Lattice Dynamics in the Harmonic Approximation*, Solid State Physics, Supplement 3 (Academic Press, New York and London, 1971), 2nd ed.
- <sup>24</sup> M. Y. Hu et al., to be published.
- <sup>25</sup> P. D. Mannheim, Phys. Rev. **165**, 1011 (1968).
- <sup>26</sup> W. Sturhahn, Hyperfine Interactions **125**, 149 (2000).
- <sup>27</sup> V. G. Kohn and A. I. Chumakov, Hyperfine Interactions **125**, 205 (2000).
- <sup>28</sup> T. S. Toellner, Hyperfine Interactions **125**, 3 (2000).
- <sup>29</sup> N. W. Ashcroft and N. D. Mermin, *Solid State Physics* (Saunders College Publishing, Fort Worth, 1976).
- <sup>30</sup> G. Simmons and H. Wang, *Single Crystal Elastic Constants and Calculated Aggregate Properties* (The M.I.T. Press, Cambridge, Massachusetts, 1971).
- <sup>31</sup> R. C. Liebermann and E. Schreiber, J. Geophys. Res. **73**, 6585 (1968).